Composition-Structure-Property-Performance Relationship in Mn-substituted $LiMn_2O_4$

C.R. Horne[1,2,*], T.J. Richardson[1], B. Gee[3], M. Tucker[1], M.M. Grush[4], U. Bergmann[1], K.A. Striebel[1], S.P. Cramer[1,5], J.A. Reimer[1,2], and E.J. Cairns[1,2]

1. Lawrence Berkeley National Laboratory, Berkeley, CA 94720
2. University of California, Berkeley, CA 94720
3. Long Island University, Brooklyn, NY 11201
4. University of Tennessee, Knoxville, TN 37996
5. University of California, Davis, CA 95616

The spinel $LiMn_2O_4$ has been extensively studied as a positive electrode active material in lithium rechargeable batteries. Partial substitution of Mn by another metal has also been the subject of recent study in an effort to improve the cycling performance. In general, the literature has shown that Mn substitution results in improved cycling stability at the expense of capacity (1,2). Resistance to the formation of tetragonal phase upon lithiation of the starting spinel (via a higher nominal Mn oxidation state in the substituted spinel) has been suggested as a mechanism for the improved performance. The degree of substitution is an important factor to optimize in order to minimize capacity loss and costs.

The spectroscopic investigations on $LiMn_2O_4$ described in the previous paper (LixMn2O4) confirmed that the cooperative Jahn-Teller effect (CJTE) from the $[Mn^{3+}O_6]$ octahedra is the mechanism for the cubic to tetragonal phase transformation. The driving force for the CJTE is based upon the electronic structure, therefore changes in electronic structure should lead to changes in the phase behavior. The fact that the

* present address: NanoGram Corporation, Fremont, CA 94538

$LiMn_{1.5}Ni_{0.5}O_4$ does not form tetragonal phase upon discharging (FUJI3, MUCK?), unlike the 100% Mn^{4+} spinel $Li_4Mn_5O_{12}$ (THAC5), led to the hypothesis that an increased degree of covalency as a source for the behavior. An increased covalence would remove the driving force for the transformation, the increased electronic stability achieved in tetragonally-distorted [$Mn^{3+}O_6$] octahedra, due to a change in electron density and widening of the Mn 3*d* bands.

The STH field is dependent upon the amount of unpaired spin density transferred between the magnetic (transition-metal) and diamagnetic ions through an intermittent oxygen ion, attributable to overlap and electron transfer effects. Therefore, the magnitude of the STH coupling constant reflects the degree of covalency (GESC@, HUAN@). In the case of $LiMn_{2-y}Me_yO_4$, the STH coupling constant characterizes the amount of unpaired spin density transferred to the Li^+ from the Mn, Co, or Ni. Similarly, the Lα/Lβ ratio of the Mn L-XES is sensitive to the amount of electron density at the Mn site as a higher ratio indicates that the Mn $3d_{5/2}$ level is more populated (GRUS1).

An investigation into the effects of Mn-substitution on the electronic structure along with the ramifications to the phase behavior upon changing lithium content was carried out. To accomplish this, a set of $LiMn_{2-y}Me_yO_4$ with Me = Li, Co, or Ni over a range of *y* were synthesized, characterized, and subjected to changes in lithium content by various techniques.

EXPERIMENTAL

Manganese-substituted spinels of the general formula $LiMn_{2-y}Me_yO_4$ were made with the following compositions: y = 0; Me = Li and y = 0.05; Me = Co and y = 0.10, 0.25, 0.50, & 1.00; Me = Ni and y = 0.05, 0.10, 0.175, 0.25, 0.33, & 0.50. $LiMn_{2-y}Me_yO_4$

spinels with $y \leq 0.25$ were synthesized using MnO_2 (CMD – IC #5, Japan Metals), $LiOH \bullet H_2O$ (Spectrum Chemical, 99.9%), along with $CoCO_3$ (Baker Reagent) or $NiCO_3$ (Alfa-AESAR, 98%) when Me = Co and Ni, respectively. Precursors were combined by grinding under *n*-hexane in a mortar and pestle. Mn-substituted spinels with $y > 0.25$ were synthesized by first jar-milling Li_2CO_3 and $MnCO_3$ (both from Baker Reagent) and either Co and Ni carbonate in acetone for 3 hours with 2 mm yttria-stabilized zirconia media (Union-Process). All combined precursors were calcined at 750°C for various times in air with intermittent grinding. Final calcination steps employed cooling at 0.8°C/min. Further details of the synthesis conditions are given in reference HORN-thesis.

Lithium extraction of $LiMn_2O_4$ to yield λ-MnO_2 and of $LiMn_{2-y}Me_yO_4$ to yield λ-$Mn_{2-y}Me_yO_4$ was performed based upon the procedure of Hunter (HUNT1). Chemical lithiation was accomplished two ways. The first method employed the reflux procedure reported in reference TARA2 using LiI whereas the second method utilized a 2.8M solution of *n*-butyl Li in hexane (Alfa-AESAR) and was performed at room temperature inside an Ar glovebox. Electrochemical lithiation was performed by discharging at 3.7 mA/g to 2.2 V, then taper discharging at 2.2 V to 1.9 mA/g, followed by further discharging at 1.9 mA/g to 2.0 V with a final taper discharging at 2.0 V until $I < 20$ µA. Once cells were discharged to the desired lithium content, x = 1.5 or 2.0 in $Li_xMn_{2-y}Me_yO_4$, the positive electrodes were extracted then washed and stored in CH_3CN inside a He glovebox until XRD scans were taken.

X-ray diffraction measurements were carried out using a Siemens D5000 diffractometer with Cu-K_α radiation over a range of 15 to 90° 2Θ for powder samples and

the range of 30 to 70° 2Θ for electrode samples. All scans were made at 0.05°, 2 sec/step. An internal Si standard was used to calibrate the 2Θ scale for powder samples whereas no standard was used for the electrode samples. Lattice parameters were determined using the programs UnitCell '96 (HOLL#) and PowderCell (ref). Further details of the experimental conditions are given in reference HORN-thesis.

Determination of the supertransferred hyperfine coupling constant was determined from measurement of the magnetic susceptibility and temperature-dependent NMR shift according to the procedure described in reference GEE1. X-ray Absorption Spectroscopy at the Mn, Co, and Ni $L_{II,III}$-edge was performed on Beamline 6.3.2 at the Advanced Light Source; procedures used for data collection and analysis are described in reference HORN-thesis. Mn L-edge XES was performed on Beamline 8.0 at the Advanced Light Source; procedures used for data collection and analysis are described in reference GRUS2.

RESULTS AND DISCUSSION

X-ray diffraction patterns of all base compositions (i.e. x = 1 in $Li_xMn_{2-y}Me_yO_4$) showed that all were cubic spinels. For the case of Me = Ni and $y \geq 0.25$ there was a small amount of intensity below the (400) reflection that has been attributed to $Li_xNi_{1-x}O$ impurity (DAHN7). Figure 1 shows the lattice parameters of the various $LiMn_{2-y}Me_yO_4$ spinels as a function of *y*. The lattice parameters of the fully-substituted spinels $LiMnCoO_4$ (8.058 Å) and $LiMn_{1.5}Ni_{0.5}O_4$ (8.170 Å) were reproducible and agree well with values reported in references KAWA# and DAHN7, respectively. Also shown in Figure 2 are linear fits for Me = Co and Me = Ni. The lattice parameter obtained for the unsubstituted material, 8.231 Å, agrees well with literature reports for similar calcination

temperature (PIST1) and precursors (THAC8). The high R-values (> 0.99) and close agreement of the y-intercepts with the lattice parameter of the unsubstituted spinel indicate that the data is of good quality. The slopes reveal that substitution of Mn with Co contracts the spinel lattice approximately 50% more than substitution with Ni.

Mn, Co, and Ni $L_{II,III}$-edge XANES was performed to determine the substituent oxidation state. Comparison of the Co and Ni spectra with divalent and trivalent model compounds revealed that Co is present as low-spin Co^{3+} whereas Ni is present as Ni^{2+} throughout the entire range of substitution. The Mn spectra for $Li_{1.05}Mn_{1.95}O_4$ along with all Me = Co and Me = Ni spinels are consistent in that they more closely resemble that of a pure Mn^{4+} compound (CRAM2) as *y* increases. Calculations have shown that $[Mn^{4+}O_6]$ octahedra are more covalent than $[Mn^{3+}O_6]$ octahedra (SHER1). Therefore, confirming the substituent oxidation state allows data to be compared on the basis of average nominal Mn oxidation state.

The data of reference GEE1 shows that the STH coupling constant increases upon substituting Li, Co, or Ni for Mn. This translates to an increased transfer of electron density to the Li ion and therefore, an increased degree of covalency. This assertion is supported by the greater STH coupling constant found for the delithiated spinel λ-MnO_2, which contains approximately 90% Mn^{4+}, as compared to $LiMn_2O_4$. Measurements of the $L\alpha/L\beta$ ratio from the Mn L-XES confirmed that the degree of covalence increases upon substitution and with increasing *y* (GRUS2). The data reveal that substitution of Mn by Li does not increase the degree of covalency as much as either Co or Ni substitution. Additionally, there is a similar effect on covalency with either Me = Co or Ni at lower degrees of substitution. The results of STH coupling constant and Mn L-XES

measurements confirm the hypothesis that Mn substitution can increase the degree of covalency within lithium manganospinels. With this information in hand the consequences of the increased covalence in $LiMn_{2-y}Me_yO_4$ to their phase behavior upon changing lithium content was explored.

As a control the volume changes associated with lithiation as well as delithiation of the unsubstituted spinel were determined and found to be in good agreement with literature reports (THAC14,OHZU1c). XRD analysis of all chemically delithiated materials showed each sample consisted of a single, cubic phase with peaks shifted to higher 2Θ. Chemical lithiation was first attempted using LiI. Subsequent XRD analysis revealed that full conversion to tetragonal phase was achieved only when $y \leq 0.10$. In contrast to the $y \leq 0.10$ spinels, some cubic phase was present in addition to the tetragonal phase when $0.10 < y \leq 0.25$ whereas cubic phase was predominant when $y \geq 0.50$. New peaks were slightly discernible in the XRD of the lithiated $LiMn_{1.5}Ni_{0.5}O_4$. The retention of cubic phase in chemically-lithiated $LiMn_{1.5}Ni_{0.5}O_4$ was first reported by Fujita *et al.* (FUJI3). However, their $LiMn_{1.5}Ni_{0.5}O_4$ discharge curves contained a plateau which is indicative of a phase transformation (MCKI1).

To verify the results for the highly substituted spinels, electrochemical lithiation by slow discharging to x = 1.5 and 2.0 in $Li_xMn_{2-y}Me_yO_4$, was performed for the five compositions y = 0; Me = Co & y = 0.50, 1.00; and Me = Ni & y = 0.33, 0.50. XRD revealed the presence of new peaks that increased in intensity with x. Additionally, the discharge curves showed that the 3-Volt insertion potential decreased in both Me = Co and Me = Ni spinels, the latter result consistent with results in reference TARA5. This indicates that the LiI solution potential was possibly not low enough for Li^+ insertion to

occur in the highly-substituted oxides. Therefore, chemical lithiation using *n*-butyl Li was performed on these same compositions.

Overlithiating the spinel (i.e. x > 2) will cause formation of Li_2MnO_2 (THAC-xs Li). To check if the the *n*-butyl Li based chemical lithiation method could result in overlithiation, $LiMn_2O_4$ was used as a control. Upon completion of the lithiation reaction, the solution on top of the reacted powder was drawn off, hydrolyzed, and then titrated with 0.1N HCl to determine residual Li^+ content. In all five cases less than 2% Li^+ was found in the liquid indicating that full insertion to $Li_2Mn_{2-y}Me_yO_4$ was attained. XRD results for the all chemically and electrochemically lithiated $LiMn_2O_4$ samples are compared in Figure 2; only tetragonal and cubic phases are present. Figure 3 compares XRD results for the chemically and electrochemically lithiated $LiMnCoO_4$ and $LiMn_{1.5}Ni_{0.5}O_4$. There is good correspondence between the new peaks among the electrochemically and *n*-butyl Li lithiated samples. Therefore, the new peaks in the highly-substituted spinels are attributed to tetragonal phase. The results show that it is important to understand the phenomenology of the lithium insertion process.

Volume changes associated with delithiation and lithiation of the $LiMn_{2-y}Me_yO_4$ were determined from the various lattice parameters and are plotted in Figure 4 (left). The data revealed that as *y* increases, the volume of delithiated cubic spinel phase increases and that of the lithiated, tetragonal spinel phase decreases. The fact that the volume of the base compositions also change with *y* make interpretation difficult. Therefore, the % change in volume, relative to the base composition, were calculated and are plotted in Figure 4 (right). This parameter is presented as a property that indicates how a material accommodates Li^+ within the structure. It is seen observed that the volume change

associated with delithiation is affected to the same degree upon substituting Mn with either Co or Ni. Conversely, the volume change associated with the transformation to tetragonal phase, or lithiation, increases for Me = Co but decreases for Me = Ni.

CONCLUSIONS

Investigations into the electronic structure of $LiMn_{2-y}Me_yO_4$ with Me = Li, Co, or Ni were conducted. It was found that Co is present in the +3 state whereas Ni is present as +2 throughout the entire range of substitution. Additionally, two different methods of characterization revealed Mn-substitution increases the degree of covalency. The covalence was not enough to suppress the CJTE-driven transformation to tetragonal phase. Electrochemical and chemical lithiation showed that, despite the changes taking place in the electronic structure, conversion to tetragonal phase occurs for compositions extending over the entire range of substitution including $LiMn_{1.5}Ni_{0.5}O_4$. Additionally, the discharge experiments showed that the 3-Volt insertion potential decreases with increasing degree of substitution.

Determinations of the volume change between the base cubic and tetragonal phases reveal that substitution with Ni improves the Li^+ accommodation of the spinel whereas substitution with Co slightly worsens it. This translates to more severe consequences for tetragonal phase formation in Me = Co spinels as compared to Me = Ni. The fact that both $LiMn_{2-y}Co_yO_4$ and $LiMn_{2-y}Ni_yO_4$ display improved cycling performance and also can ameliorate tetragonal phase formation during cycling (BITO1, LIU3) is attributed to the fact that the 3-Volt insertion potential is lowered upon substitution. The lower insertion potential means that a greater driving force is required to form the tetragonal phase.

ACKNOWLEDGEMENTS

The work at Lawrence Berkeley National Laboratory was supported by the Director, Office of Energy Research, Office of Basic Energy Sciences, Chemical Sciences Division of the U.S. Department of Energy under Contract No. DE-AC03-76SF00098 to the Ernest Orlando Lawrence Berkeley National Laboratory.

REFERENCES

1. R.J. Gummow, A. de Kock, and M.M. Thackeray, Sol. St. Ionics. **69**, 59 (1994).

2. L. Guohua, T. Uchida, and M. Wakihara, J. Electrochem. Soc., **143**, 178 (1996).

BITO1. Y. Bito, H. Murai, S. Ito, M. Hasegawa, and Y.A. Toyoguchi, in Proceedings of the Symposium on Rechargeable Lithium and Lithium-Ion Batteries, The Electrochemical Society PV 94-28, p. 461, 1994.

CRAM2. S.P. Cramer, F.M.F. deGroot, Y. Ma, C.T. Chen, F. Sette, C.A. Kipke, D.M. Eichhorn, M.K. Chan, W.H. Armstrong, E. Libby, G. Christou, S. Brooker, V. McKee, O.C. Mullins, and J.C. Fuggle, *J. Am. Chem. Soc.*, **113**, 7937 (1991).

DAHN7. Q. Zhong, A. Bonakdarpour, M. Zhang, Y. Gao, and J.R. Dahn, J. Electrochem. Soc., **144**, 205 (1997).

FUJI3. K. Amine, H. Tukamoto, H. Yasuda, and A. Fujita, *J. Electrochem. Soc.*, **143**(1996)1607.

GEE1. B. Gee, C.R. Horne, E.J. Cairns, and J.A. Reimer, J. Phys. Chem. B, **102**, 10142 (1998).

GESC@. S. Geschwind in *Hyperfine Interactions*, A.J. Freeman and R.B. Frankel, eds., Academic Press, New York, 1967.

GRUS1. M.M.Grush, Y. Muramatsu, J.H. Underwood, E.M.. Gullikson, D.L. Ederer, R.C.C. Perera, T.A. Callcot, *J. Elect. Spect.* **1998** 92, 225.

GRUS2. M.M.Grush, C.R.Horne, R.C.C. Perera, D.L. Ederer, S.P. Cramer, E.J. Cairns, T.A. Callcott, submitted to *Chem. Mat.*

HOLL#. T.J.B. Holland and S.A..T. Redfern, *Mineralogical Magazine*, **61**(1997)65.

HORN-thesis. C.R. Horne, PhD Dissertation, in prep. (1999).

HUAN@. N.L. Huang, R. Orback, E. Simnek, J. Owen, and D.R. Taylor, *Phys. Rev. B*, **37**(1988)9140.

HUNT1. J.C. Hunter, *J. Sol. State Chem.*, **39**(1981)142-147.

KAWA#. H. Kawai, M. Nagata, H. Tukamoto and A. R. West, *Electrochem. and Sol. State Lett.*, **1** (1998) 212.

LIU3. W. Liu, K. Kowal, and G.C. Farrington, *J. Electrochem. Soc.*, **143**(1996)3590.

LixMn2O4. C.R. Horne, U. Bergmann, M.M. Grush, J. Kim, A. Manthiram, S.P. Cramer, K.A. Striebel, and E.J. Cairns

OHZU1c. T. Ohzuku, M. Kitagawa, and T. Hirai, *J. Electrochem. Soc.* **137**(1990)769.

MCKI1. W.R. McKinnon and R.R. Haering, *Physical Mechanisms of Intercalation* in Modern Aspects of Electrochemistry, v. 15, R.E. White, J. O'M. Bockris, and B.E. Conway, eds. Plenum Press, NY, p. 235 304 (1983).

PCEL.

PIST1. G. Pistoia and G. Wang, *S.S.Ionics* **66**(1993)135-142.

SHER1. D.M. Sherman, *Am. Miner.*, **69**(1984)788.

TARA2. J. M. Tarascon and D. Guyomard, *J Electrochem. Soc.* **138**(1991)2864.

TARA5. J.M. Tarascon, E. Wang, F.K. Shokoohi, W.R. McKinnon, and S. Colson, *J. Electrochem. Soc.*, **138**(1991)2859.

THAC5. M.M. Thackeray, A. de Kock, M.H. Rossouw, D.C. Liles, R. Bittihn, and D. Hoge, *J. Electrochem. Soc.*, **139**(1993)363.

THAC14. J.B. Goodenough, M.M. Thackeray, W.I.F. David and P.G. Bruce, *Rev. de Chem. Min.* **21**(1984)435.

THACxsvLi. W. I. F. David, J. B. Goodenough, M. M. Thackeray, and M. G. S. R. Thomas, *Rev. de Chem. Min.* **20**(1983)636-642.

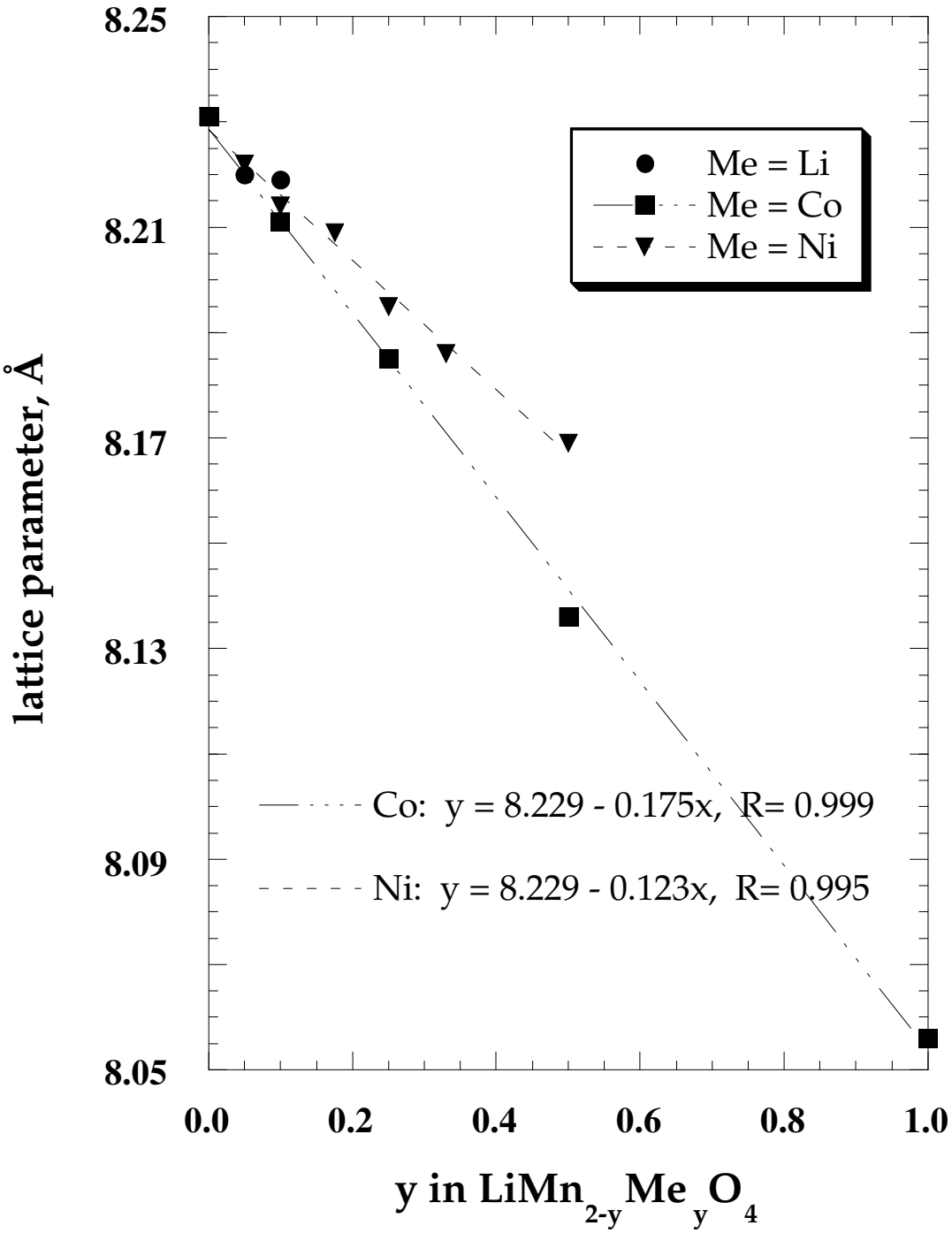

Figure 1. Lattice parameters for $LiMn_{2-y}Me_yO_4$.

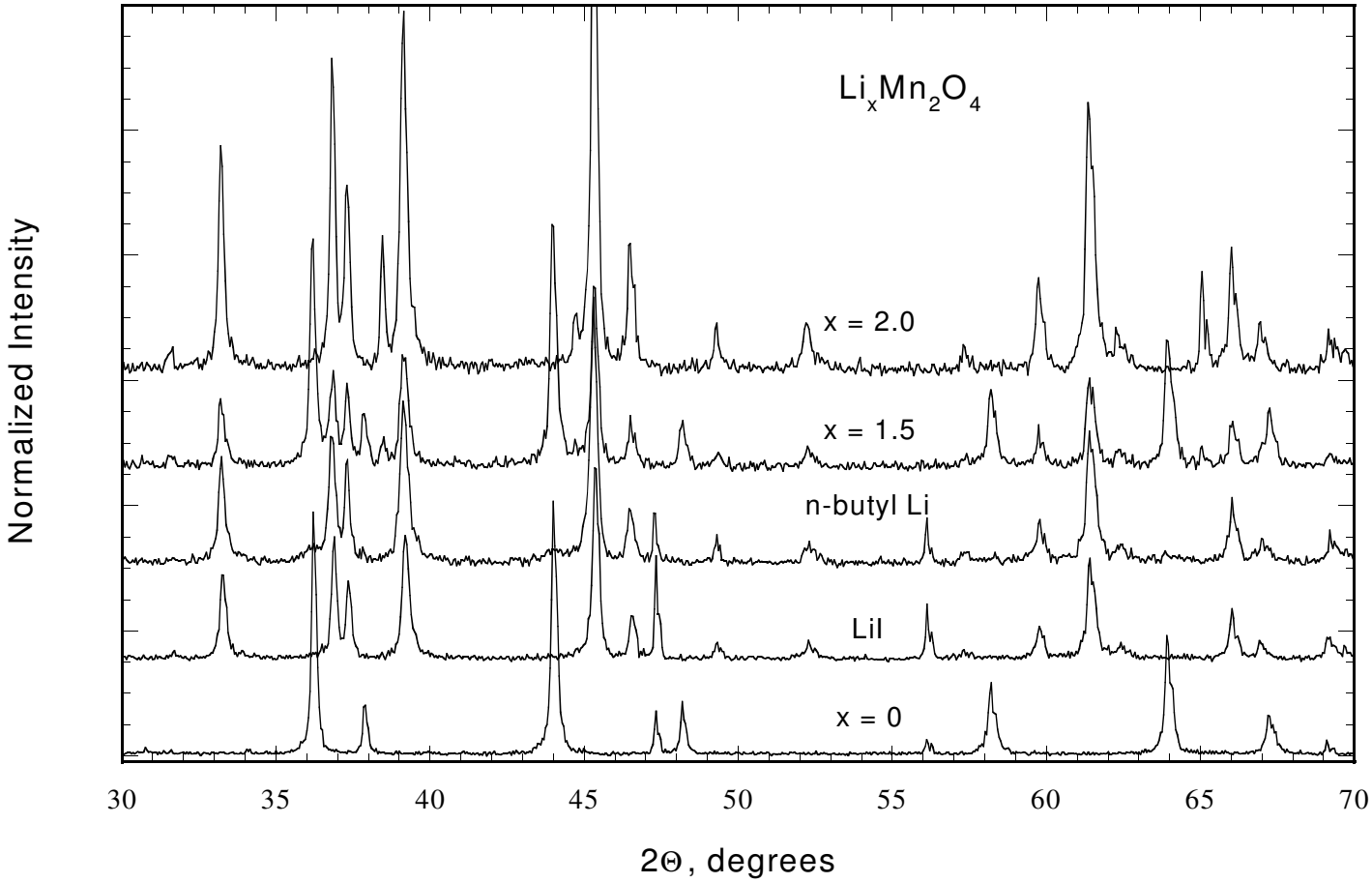

Figure 2. XRD patterns of $LiMn_2O_4$ and lithiated derivatives prepared using LiI, *n*-butyl Li, and electrochemically.

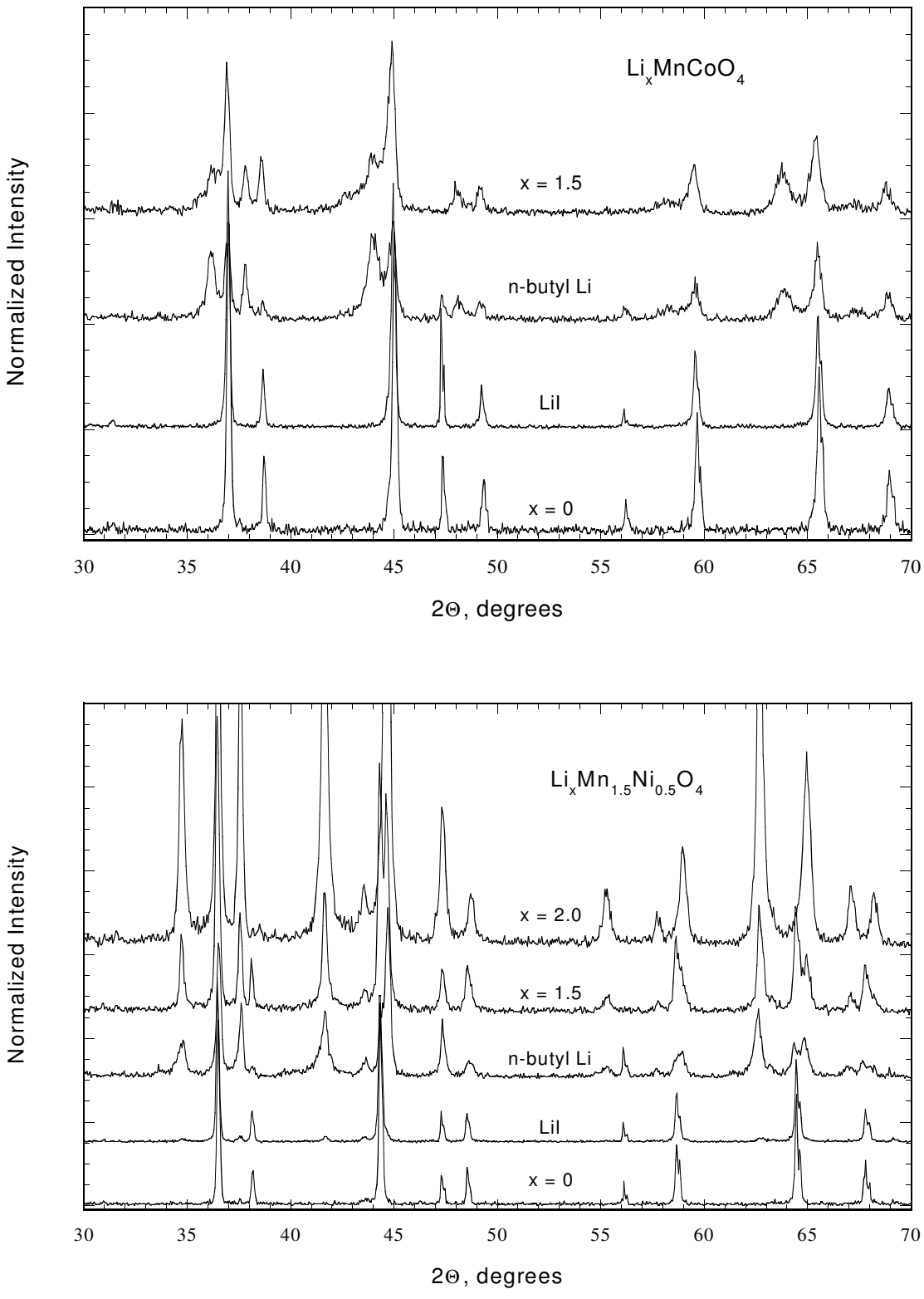

Figure 3. XRD patterns of $LiMnCoO_4$ (top) and $LiMn_{1.5}Ni_{0.5}O_4$ (bottom) along with their lithiated derivatives prepared using LiI, *n*-butyl Li, and electrochemically.

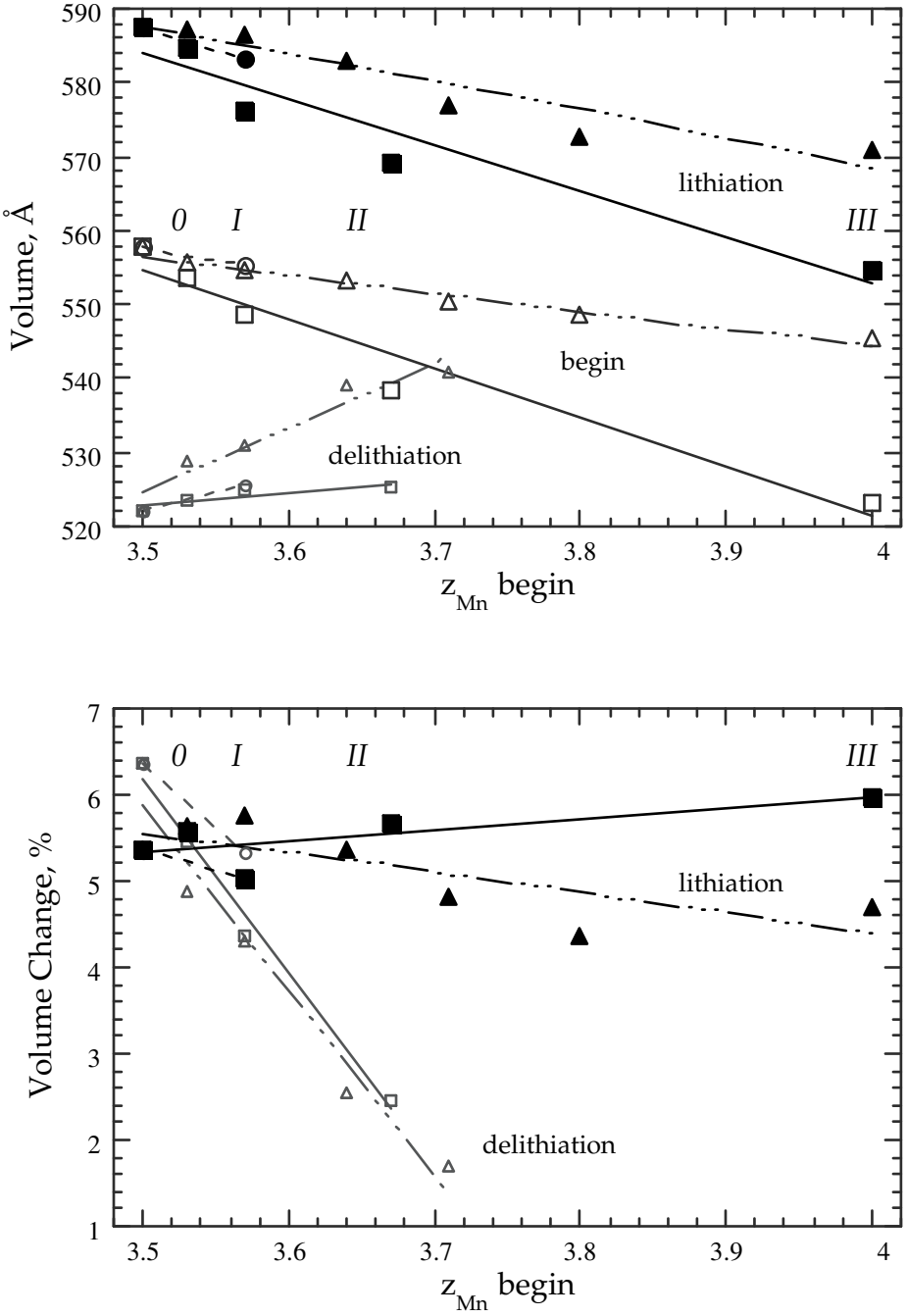

Figure 4. Volume change (top) and % volume change (bottom) for $LiMn_{2-y}Me_yO_4$ as a function of lithium content and composition. Circles represent Me = Li, squares represent Me = Co, and triangles represent Me = Ni. Small symbols are used for delithiated compounds whereas filled symbols represent lithiated compounds.